Phosphomevalonate Kinase: Functional Investigation of the Recombinant Human Enzyme†

Timothy J. Herdendorf and Henry M. Miziorko*

Division of Molecular Biology and Biochemistry, School of Biological Sciences, University of Missouri−Kansas City, Kansas City, Missouri 64110

Received November 1, 2005; Revised Manuscript Received January 16, 2006

ABSTRACT: Phosphomevalonate kinase (PMK) catalyzes a key step in isoprenoid/sterol biosynthesis, converting mevalonate 5-phosphate and ATP to mevalonate 5-diphosphate and ADP. To expedite functional and structural study of this enzyme, an expression plasmid encoding His-tagged human PMK has been constructed and recombinant enzyme isolated in an active, stable form. PMK catalyzes a reversible reaction; kinetic constants of human PMK have been determined for both forward (formation of mevalonate 5-diphosphate) and reverse (formation of mevalonate 5-phosphate) reactions. Animal and invertebrate PMKs are not orthologous to plant, fungal, or bacterial PMKs, limiting the information available from sequence alignment analysis. A homology model for the structure of human PMK has been generated. The model conforms to a nucleoside monophosphate kinase family fold. This result, together with sequence comparisons of animal and invertebrate PMKs, suggests an N-terminal basic residue rich sequence as a possible "Walker A" ATP binding motif. The functions of four basic (K17, R18, K19, K22) residues and one acidic (D23) residue in the conserved sequence have been tested by mutagenesis and characterization of isolated mutant proteins. Substrate K_m values for K17M, R18Q, K19M, and D23N have been measured for forward and reverse reactions; in comparison with wild-type PMK values, only modest (<12-fold) changes are observed. In contrast, R18Q exhibits a V_{max} decrease of 100/300-fold (forward/reverse reaction). K22M activity is too low for measurement at nonsaturating substrate concentration; specific activity is decreased by >10000-fold in both forward/reverse reactions, suggesting an active site location and an important role in phosphoryl transfer.

Phosphomevalonate kinase (PMK;[1] EC 2.7.4.2) catalyzes the reversible ATP-dependent phosphorylation of mevalonate 5-phosphate to produce mevalonate diphosphate and ADP:

mevalonate 5-phosphate + ATP ⇄ mevalonate 5-diphosphate + ADP

The reaction represents a key step in the mevalonic acid mediated biosynthesis of isopentenyl diphosphate and other polyisoprenoid metabolites. Mammalian phosphomevalonate kinase has not been extensively characterized in comparison with other enzymes of mammalian isoprenoid and cholesterol biosynthesis. Enzyme activity was documented in pig liver (*1*), and the porcine enzyme has been isolated and partially characterized (*2*, *3*). In recent years, accumulation of the PMK reaction product, mevalonate diphosphate, has been implicated in the inhibition and coordinate regulation of cholesterol and fatty acid biosynthesis in liver cells (*4*). The sequence of human PMK has been deduced (*5*), and expression of a GST-human PMK fusion construct (*6*) has produced protein used for some preliminary characterization work.

Analysis of the rapidly expanding genomic database indicates that animal PMKs and low-homology invertebrate PMKs are encoded by genes that are nonorthologous to plant, fungal, and bacterial PMK genes (*7*). The recent discovery of the mevalonate pathway for isoprenoid biosynthesis in Gram-positive cocci (*8*) has been a prelude to expression of a recombinant *Streptococcus pneumoniae* enzyme, which has been crystallized and used for elucidation of a protein structure (*9*). The fold of this nonorthologous protein confirms it as a member of the GHMP kinase (galactokinase/homoserine kinase/mevalonate kinase/phosphomevalonate kinase) family. Additionally, this prokaryotic enzyme has been kinetically characterized (*10*). No empirical structural information is available for the divergent animal PMK proteins.

To facilitate a more detailed understanding of mevalonate diphosphate synthesis in humans, availability of substantial amounts of a stable form of recombinant human PMK would be valuable. This report describes the development of a highly efficient expression system for human PMK, as well as isolation and characterization of the active, stable enzyme. A homology model for human PMK structure has been generated, providing a structural rationale for inclusion of PMK in the nucleoside monophosphate kinase family of phosphotransferases. Such a prediction is compatible with

† This work was supported in part by the NIDDK.

* Address correspondence to this author. E-mail: miziorkoh@umkc.edu. Phone: 816-235-2246. Fax: 816-235-5595.

[1] Abbreviations: PMK, phosphomevalonate kinase; MVP, mevalonate 5-phosphate; MVPP, mevalonate 5-diphosphate; TNP-ATP, 2′-(3′)-*O*-(2,4,6-trinitrophenyl)adenosine 5′-triphosphate; DNK, deoxynucleotide kinase; PHYRE, Protein Homology/analogY Recognition Engine.

10.1021/bi052231u CCC: $33.50
Published on Web 02/18/2006

results of recent large-scale analyses of phosphotransferase protein sequences (*11*). The homology model, as well as similarities between amino acid sequences of PMK and other phosphotransferases, can guide the design of functional tests of PMK amino acids predicted to map within the catalytic site. The results of the first functional tests of human PMK active site residues are presented and interpreted in the context of the chemistry of phosphoryl transfer.

MATERIALS AND METHODS

Materials. Deoxynucleotides used for cloning were purchased from Operon Technologies, Inc. PCR amplification of DNA utilized Pfu DNA polymerase purchased from Stratagene. Restriction enzymes and T4 DNA ligase were obtained from New England Biolabs and Fisher Scientific. Plasmid DNA was propagated in *Escherichia coli* JM109 cells (Promega). Kits for plasmid DNA purification were purchased from Eppendorf (miniprep) and Qiagen (midiprep). Gel-purified DNA fragments were purified using the Qiaquick gel extraction kit (Qiagen). Plasmids used for subcloning were purchased from Novagen. DNA sequencing was performed at the Protein and Nucleic Acid Shared Facility (Medical College of Wisconsin). *E. coli* BL21(DE3) Rosetta cells were obtained from Novagen. Isopropyl β-D-thiogalactopyranoside (IPTG) was purchased from Research Products Corp. Ni−Sepharose was purchased from GE Healthcare. Imidazole was purchased from Lancaster Synthesis Inc. 2′(3′)-*O*-(2,4,6-Trinitrophenyl)adenosine 5′-triphosphate (TNP-ATP) was obtained from Molecular Probes. Potassium phosphates (KP_i), 3-morpholinopropanesulfonic acid (MOPS), dithiothreitol (DTT), potassium chloride (KCl), magnesium chloride ($MgCl_2$), media components, and antibiotics were purchased from Fisher Scientific. All other biochemical reagents and coupling enzymes were purchased from Sigma Chemical Co.

Synthesis of Mevalonate 5-Phosphate and Mevalonate 5-Diphosphate. The syntheses of mevalonate 5-phosphate and mevalonate 5-diphosphate have been previously reported (*12*, *13*) and are briefly summarized. Methyl 3-hydroxy-3-methyl-5-iodopentanoate was synthesized using the method of Reardon and Abeles (*13*) by reacting mevlonolactone with trimethylsilyl iodide, followed by diazomethane derivatization to form the methyl ester, which was subsequently purified by silica gel chromatography. Methyl 5-phosphomevalonate was synthesized by reacting the purified methyl 3-hydroxy-3-methyl-5-iodopentanoate with an excess of tetrabutylammonium phosphate. The methyl 5-phosphomevalonate was converted to the lithium salt by passage over a Dowex 50 column (lithium form). Deesterification was accomplished by alkaline hydrolysis in 0.5 N LiOH. The resulting mevalonate 5-phosphate was purified by anion-exchange chromatography using a DEAE-Sephadex A25 column. The chromatographically purified product was then analyzed, and the concentration of the physiologically active *R* isomer was determined by enzymatic end point assay. Mevalonate 5-diphosphate was synthesized in a similar manner, but tetrabutylammonium pyrophosphate was used as the phosphorylation reagent.

Plasmid Construction and Protein Expression. The open reading frame encoding human PMK (generously supplied by Dr. K. M. Gibson as a glutathione *S*-transferase fusion construct) was subcloned into the expression plasmid pET15b using standard molecular biology techniques. Briefly, the gene was amplified by polymerase chain reaction using primers complementary to the 5′ and 3′ region of the gene. The 5′ primer (5′-AAGGAGATATACAT**ATG**GCCCCGCTGGGAGGCGC-3′) encoded an *Nde*I site (underscored) harboring the ATG (boldface) start codon; the 3′ primer (5′-CAGTGGTGGTGGTGGGGATC**CTA**AAGTCTGGAGC-3′) encoded a *Bam*HI site (underscored) downstream of the stop codon (boldface). The amplified cDNA and pET15b were digested with the appropriate restriction enzymes and gel purified. The purified DNA was ligated with *Nde*I/*Bam*HI-digested vector overnight at 4 °C. The ligation product represents an expression construct that encodes human PMK containing an N-terminal His_6 affinity tag and was designated pTH202. The integrity of the gene was verified by DNA sequence analysis. Chemically competent *E. coli* BL21(DE3) Rosetta cells were transformed with the pTH202 construct. The transformed cells were plated onto LB agar containing ampicillin (amp) and chloramphenicol (cam). These plates were incubated overnight at 37 °C. Two milliliters of LB−amp−cam was inoculated with a single colony and allowed to grow to moderate turbidity ($A_{600} \sim 0.3$). This culture was used to inoculate 20 LB−amp−cam plates (100 μL/plate). The plates were incubated overnight at 37 °C. The resulting lawns were used to inoculate 500 mL of LB−amp−cam. The liquid culture was incubated at 30 °C for 1 h and induced with 1 mM IPTG. The culture was harvested 4 h postinduction by centrifugation.

Mutagenesis. A full-circle PCR method, which employed a Stratagene QuikChange site-directed mutagenesis protocol, was used to generate the desired mutations. The presence of the mutation and the integrity of the remaining coding sequence were verified by DNA sequencing. Primer sequences used in the mutagenic reactions are as follows: K17M forward, 5′-GCTGTTCAGCGGC**ATG**AGGAAATCCGGGAAG-3′, K17M reverse, 5′-CTTCCCGGATTTCCT-**CAT**GCCGCTGAACAGC-3′; R18Q forward, 5′-GTTCAGCGGCAAG**CAG**AAATCCGGGAAGGACTTC-3′, R18Q reverse, 5′-GAAGTCCTTCCCGGATTT**CTG**CTTGCCGCTGAAC-3′; K19M forward, 5′-CAGCGGCAAGAGG**ATG**TCCGGGAAGGACTTCG-3′, K19M reverse, 5′-CGAAGTCCTTCCCGGA**CAT**CCTCTTGCCGCTG-3′; K22M forward, 5′-GAGGAAATCCGGG**ATG**GACTTCGTGACC-3′, K22M reverse, 5′-GGTCACGAAGTC-**CAT**CCCGGATTTCCTC-3′; D23N forward, 5′-GGAAATCCGGGAAG**AAC**TTCGTGACCGAG-3′, D23N reverse, 5′-CTCGGTCACGAA**GTT**CTTCCCGGATTTCC-3′.

Enzyme Purification. Bacterial pellets were resuspended in 100 mL of buffer containing 50 mM KP_i, 100 mM KCl, 5 mM imidazole, and 0.5 mM DTT at pH 7.8. Lysis was accomplished by passage through a microfluidizer at ~17 kpsi. The lysate was clarified by centrifugation at ~100000*g* and the supernatant loaded onto ~1 mL of Ni−Sepharose Fast-Flow resin. The column was washed with the lysis buffer until $A_{280} < 0.005$, and the protein was eluted using the lysis buffer supplemented with 300 mM imidazole. The fractions containing PMK were pooled, and the concentration was determined spectrophotometrically using an extinction coefficient ($\epsilon_{280} = 32290\ M^{-1}\ cm^{-1}$) calculated from the deduced protein composition.

Estimation of the Molecular Mass of Human Phosphomevalonate Kinase. The molecular mass of native human PMK was estimated by size exclusion chromatography using a Superdex 75 HR 10/30 (GE Healthcare) run at 0.5 mL/min in 100 mM MOPS, 150 mM KCl, and 1 mM DTT at pH 7.0 using an Akta protein purification system (GE Healthcare). A total of ~0.3 mg of each of six protein standards (ovalbumin, 45 kDa; carbonic anhydrase, 29 kDa; chymotrypsinogen, 24 kDa; myoglobin, 17 kDa; cytochrome *c*, 12.5 kDa; and aprotinin, 6.5 kDa) and purified PMK were individually loaded in a 100 μL volume via a 100 μL sample loop. Blue Dextran was used to determine the void volume of the column, and K_{av} was determined using the formula K_{av} = (elution volume − void volume)/(column volume − void volume). The K_{av} was plotted versus the log molecular mass of the standards, a molecular mass for human PMK was estimated using the standard curve generated by the standards, and the K_{av} was measured for PMK. The subunit molecular mass of human PMK was estimated by denaturing SDS−PAGE using appropriate molecular mass standards (*14*).

Steady-State Kinetics. For measurement of enzyme activity, a coupled enzyme assay was employed (*15*, *16*). In the forward reaction, initial velocities were determined by coupling the production of ADP to the oxidation of NADH with pyruvate kinase/lactate dehydrogenase (3 units per assay), and rate of decrease in absorbance at 340 nm was monitored. In the reverse reaction, activity was determined by coupling the production of ATP to the reduction of $NADP^+$ with hexokinase/glucose-6-phosphate dehydrogenase (3 units per assay), and the rate of increase in absorbance at 340 nm was monitored. Spectrophotometric measurements were done using a Lambda 35 spectrophotometer (Perkin-Elmer). Catalytically impaired mutants were assayed fluorometrically using an excitation wavelength of 340 nm and monitoring the rate of change in the emission wavelength of 460 nm for the fluorophore (NADH or NADPH) using a Photon Technologies International spectrofluorometer. The activity of WT PMK was also determined fluorometrically and was in good agreement with estimates measured spectrophotometrically. All assays were started with the addition of mevalonate 5-phosphate in the forward reaction and mevalonate 5-diphosphate in the reverse reaction. For estimates of maximum velocity (V_{max}) and Michaelis constant (K_m), the reaction velocities at various substrate concentrations were fit to the Michaelis−Menten equation using the Kaleidagraph graphing and data analysis software (Synergy Software, Reading, PA). All assays were done at 30 °C in the presence of 100 mM MOPS, 200 mM KCl, 1 mM DTT, and 10 mM $MgCl_2$ at pH 7.0. One unit of activity corresponds to 1 μmol of substrate converted to product in 1 min.

TNP-ATP Binding to Wild-Type and Mutant PMK Proteins. The recombinant wild-type and mutant enzymes were tested for active site structural integrity using TNP-ATP, a fluorescent analogue of ATP. TNP-ATP was titrated into buffer alone or into buffer containing a fixed concentration of enzyme. The buffer used for these fluorescence measurements was 100 mM MOPS, 100 mM KCl, and 1 mM DTT at pH 7.0. The excitation wavelength used in these experiments was 409 nm. Emission spectra were scanned from 500 to 600 nm, using a 5 nm slit width. TNP-ATP concentration was determined by absorbance at 409 nm using the extinction coefficient of 26400 M^{-1} cm^{-1} (*17*). For data analysis, values measured at the fluorescent emission peak of 533−535 nm for bound probe were corrected for free TNP-ATP/buffer and for any scattering that occurred. Thus, these corrected fluorescence enhancement data were plotted against TNP-ATP concentrations and analyzed by nonlinear regression to yield dissociation constants (K_d) and extrapolated maximum binding (B_{max}). Binding stoichiometries were estimated by dividing the B_{max} by the product of the enzyme concentration used for the experiment and the fluorescence enhancement corresponding to 1 μM enzyme-bound probe.

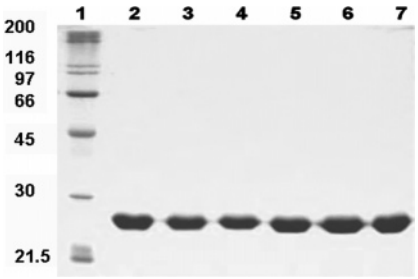

FIGURE 1: SDS−PAGE of wild-type and mutant human PMKs. Lane 1: molecular mass markers (myosin, 200 kDa; β-galactosidase, 116 kDa; phosphorylase *b*, 97 kDa; serum albumin, 66 kDa; ovalbumin, 45 kDa; carbonic anhydrase, 30 kDa; trypsin inhibitor, 21.5 kDa). Lanes 2−7 contain 10 μg of human PMK proteins corresponding to wt, K17M, R18Q, K19M, K22M, and D23Q, respectively.

Homology Modeling of Human Phosphomevalonate Kinase. The sequence of human PMK was submitted for analysis by the PHYRE protein homology/analogy recognition engine (http://www. sbg.bio.ic.ac.uk/~phyre/). The PHYRE homology model method employs a 3D-position-specific scoring matrix (*18*) and is benchmarked using remotely homologous proteins with less than 30% identity. High probability scores (4.3 e−06; 95% probability in the case of the human PMK model) suggest that the query protein is homologous to the structure used for generation of the model and that the query protein (e.g., human PMK) belongs to the same SCOP superfamily. The quality of the resulting homology model was evaluated (e.g., bond angles, lengths) by using the PDB file for analysis by PROCHECK (*19*).

RESULTS

Characterization of Recombinant Human Phosphomevalonate Kinase. Initial attempts at protein expression involved use of pET23d for construction of an expression plasmid encoding enzyme with a histidine tag after the C-terminus. This strategy supported production of active enzyme, but a modest level of expression was achieved. Isolation of approximately 5 mg of enzyme/L of bacterial culture is supported using this approach. A more productive method involves use of pET15b for construction of enzyme with the histidine tag upstream of the N-terminus of human PMK. Soluble enzyme is expressed as a substantial component (~10%) of total *E. coli* protein, and isolation in homogeneous form using a Ni−Sepharose resin (Figure 1) results in a substantial improvement (>25 mg/0.5 L of bacterial culture) in yield. Specific activity (52 units/mg) is comparable to C-tagged enzyme and is approximately 20-fold higher than reported (*6*) for a GST-human PMK fusion protein. IPTG-

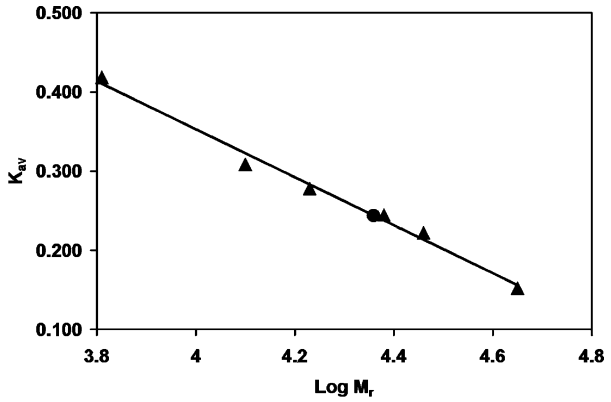

FIGURE 2: Analytical gel filtration of recombinant human PMK under nondenaturing conditions. Chromatography was performed using a Superdex 75 HR 10/30 (1 × 30 cm) column. The figure depicts the elution properties of PMK (●) and various molecular mass standards (▲): ovalbumin, 45 kDa; carbonic anhydrase, 30 kDa; chymotrypsinogen, 24 kDa; myoglobin, 17 kDa; cytochrome *c*, 12.5 kDa; aprotinin, 6.5 kDa. Protein samples (300 μg) were loaded on the column and eluted with 100 mM MOPS, 150 mM KCl, and 1 mM DTT (pH 7.0). K_{av} was determined using the formula: (elution volume − void volume)/(column volume − void volume). The void volume was determined using blue dextran. The column volume estimate is specified by the manufacturer.

induced expression at 30 °C produces enzyme that, after isolation, is stable for at least 1 week at ambient temperature.

A subunit molecular mass of 27.5 kDa for recombinant human PMK is estimated under SDS−PAGE conditions (Figure 1); this estimate is slightly larger than the molecular mass (24.2 kDa) deduced from the amino acid sequence of the His-tagged protein. Analytical size exclusion chromatography experiments under nondenaturating conditions (Figure 2) indicate a molecular mass of ~22.9 kDa, suggesting that native human PMK exists as a monomer. In this respect, the human enzyme is comparable to PMK protein isolated from pig liver (*2*, *3*).

Kinetic Properties of Human Phosphomevalonate Kinase. Analysis of the rate of enzymatic production of mevalonate diphosphate and ADP indicates a V_{max} for recombinant human PMK (52 units/mg) that is comparable to enzyme from animal tissue. Apparent K_m values of 34 and 107 μM for mevalonate 5-phosphate and MgATP, respectively (Table 1), are in good agreement with reported K_m values for the human GST-PMK fusion protein (*6*). The reported K_m values for the pig liver enzyme vary considerably for both mevalonate 5-phosphate and ATP, ranging from 20 to 300 μM mevalonate 5-phosphate and 56−550 μM ATP (*2*, *3*, *6*, *20*), possibly reflecting differences in assay conditions and buffers. K_m values measured for the human PMK fall within this broad range.

While PMK catalyzes a reversible reaction (*1*, *10*, *21*−*23*), kinetic parameters for production of mevalonate 5-phosphate and ATP have not been reported for eukaryotic enzyme. In this reverse reaction, the recombinant human enzyme exhibits a V_{max} of 12 units/mg and apparent K_m values of 41 and 47 μM for mevalonate 5-diphosphate and ADP, respectively (Table 2).

Strategies for Selection of Enzyme Residues for Tests of Contribution to Active Site Function. The utility of a sequence homology approach to identify conserved regions of PMK sequence is limited by the availability of information for only a few animal and invertebrate proteins, a sharp contrast with the larger database available for plant, fungal, and bacterial PMK proteins. Despite this constraint, it is possible to identify near the proteins' N-termini (Figure 3) a highly conserved region (residues 16−23: GKRKSGKD) which is highly basic (K17, R18, K19, K22) in composition. It has been proposed (*11*) that this basic sequence represents an ATP binding motif, although the multiplicity of basic residues and the presence of an invariant aspartate (D23) instead of T/S at the C-terminus of this sequence are not typical. However, the bacteriophage T4 deoxynucleotide

Table 1: Kinetic Constants of Wild-Type and Mutant Phosphomevalonate Kinases Determined for the Forward Reaction[a]

enzyme	$K_{m(R-MVP),app}$ (μM)	$V_{max(R-MVP)}$ (units/mg)	$K_{m(MgATP),app}$ (μM)	$V_{max(MgATP)}$ (units/mg)
WT	34 ± 3	46.4 ± 1.0	107 ± 14	52.0 ± 1.1
K17M	176 ± 30	6.6 ± 0.4	556 ± 79	6.6 ± 0.2
R18Q	123 ± 12	0.55 ± 0.02	536 ± 103	0.59 ± 0.04
K19M	230 ± 36	5.5 ± 0.3	1312 ± 147	5.5 ± 0.2
K22M[b]	nd	nd	nd	0.00066 ± 0.00012
D23N	116 ± 13	7.2 ± 0.2	815 ± 62	6.7 ± 0.2

[a] Spectrophotometric assays were performed in 100 mM MOPS, 200 mM KCl, and 1 mM DTT (pH 7.0) in the presence of 10 mM $MgCl_2$ at 30 °C. Values were determined by fitting the data to a Michaelis−Menten equation. Errors represent the standard error of the fit. [b] Specific activity determination under standard conditions using a fluorescence assay with the same buffer conditions. Error represents the standard deviation of six measurements. nd indicates not determined.

Table 2: Kinetic Constants of Wild-Type and Mutant Phosphomevalonate Kinases Determined for the Reverse Reaction[a]

enzyme	$K_{m(R-MVPP),app}$ (μM)	$V_{max(R-MVPP)}$ (units/mg)	$K_{m(MgADP),app}$ (μM)	$V_{max(MgADP)}$ (units/mg)
WT	41 ± 3	11.3 ± 0.2	47 ± 5	12.0 ± 0.2
K17M	187 ± 34	2.2 ± 0.1	286 ± 16	2.0 ± 0.1
R18Q	47 ± 5	0.040 ± 0.001	65 ± 3	0.044 ± 0.001
K19M	79 ± 12	0.12 ± 0.01	131 ± 17	0.12 ± 0.01
K22M[b]	nd	nd	nd	0.00035 ± 0.00004
D23N	138 ± 14	0.27 ± 0.01	79 ± 10	0.30 ± 0.01

[a] Spectrophotometric assays were performed in 100 mM MOPS, 200 mM KCl, and 1 mM DTT (pH 7.0) in the presence of 10 mM $MgCl_2$ at 30 °C. Values were determined by fitting the data to a Michaelis−Menten equation. Errors represent the standard error of the fit. [b] Specific activity determination under standard conditions using a fluorescence assay with the same buffer conditions. Error represents the standard deviation of six measurements. nd indicates not determined.

```
                                  10         20         30
                          ....|....| ....|.***| .**.|....|
H. sapiens PMK            MAPLGGAPRL VLLFSGKRKS GKDFVTEALQ
M. musculus PMK           MAPLGASPRL VLLFSGKRKS GKDFVTERLK
S. scrofa PMK             MAPLGSVPRL VLLFSGKRKD GKDFVTEALQ
R. norvegicus PMK         MAPLGASPRL VLLFSGKRKS GKDFVTERLQ
D. rerio PMK              MATT--QPSI ILLFSGKRKS GKDYVTDLIQ
C. briggsae PMK           ------MVKF VIAISGKRKS GKDYCTNKLI
C. elegans PMK            -------MPI VIAISGKRKS GKDYCTNLIR
D. pseudoobscura PMK      ------MLKI VLI-SGKRKC GKDYISERLQ
D. melanogaster PMK       ------MMKI VLI-SGKRKC GKDYISERLQ
```

FIGURE 3: Sequence alignment of the N-terminal region of animal/invertebrate phosphomevalonate kinases. The putative "Walker A" phosphate binding loop is shown in bold letters. All sequences were obtained from public databases. Alignment was generated using the BioEdit program (*37*). Asterisks indicate residues mutated in *H. sapiens* PMK. Sequences correspond to the following organisms and accession numbers: *H. sapiens* (human), Q15126; *M. musculus* (mouse), NP_081060; *D. rerio* (zebra fish), XM_680509.1; *R. norvegicus* (rat), NP_001008353; *S. scrofa* (pig), Q29081; *C. briggsae* (nematode), CAE64922; *C. elegans* (flatworm), CAD66220; *D. psuedoobscura* (fruit fly), EAL34326; *D. melanogaster* (fruit fly), AAF53833.

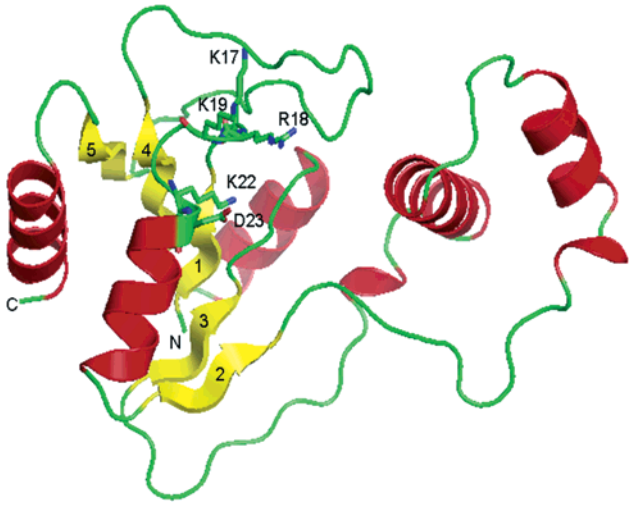

FIGURE 4: Homology model of *H. sapiens* phosphomevalonate kinase. The model was created using the PHYRE algorithm (*18*) and is based on threading the human PMK sequence on the backbone of the bacteriophage T4 deoxynucleotide kinase structure (*24*). Residue side chains targeted for mutagenesis are displayed.

kinase sequence provides an example of such an acidic group at the end of an ATP binding loop.

Another method of analyzing human PMK protein has become available by using the PHYRE algorithm (*18*) to generate a homology model of this protein's three-dimensional structure. The PHYRE homology model method is benchmarked using remotely homologous proteins with less than 30% identity. High probability scores (95% probability in the case of the human PMK model) suggest that the query protein is homologous to the structure used for generation of the model and that the query protein (e.g., human PMK) belongs to the same SCOP superfamily. The homology model is not a substitute for an empirically determined structure but is intended for use as a guide to the design of experiments and functional tests. Analysis of the PMK model (159 residues) was performed to produce a Ramachandran plot in which, out of 143 non-glycine and non-proline residues, 141 fall into allowed regions, 2 fall into generously allowed regions, and none fall into the disallowed region. Only two main chain bond lengths differ by >0.05 Å from typical small molecule values. Only four main chain bond angles differ by >10 deg from typical small molecule values. These deviations from typical parameters for these few main chain bonds do not influence the putative N-terminal ATP binding loop region of the PMK model. The model is based on threading the human PMK sequence onto the backbone of bacteriophage T4 deoxynucleotide kinase (*24*). Thus, the model predicts that human PMK adopts the fold of the nucleoside monophosphate kinase family of proteins. The model (Figure 4) spans residues 11−186 of the 192-residue human PMK protein, with gaps corresponding to residues 127−128 and 140−149. The core of the structure is a sheet of five parallel β strands. Situated above the β sheet core are two less structured regions (following β strands 2 and 4) that correspond to the "lid" domains that are characteristics of nucleoside monophosphate kinase family enzymes. The loop following strand 1 (the middle strand in the sheet) corresponds to the conserved basic sequence described above. At the C-terminal end of the adjacent β strand 3 are four hydrophobic residues followed by invariant S107 and D108. Properties of these polar side chains and proximity to a putative ATP binding loop suggest that this region represents a "Walker B" motif usually associated with binding of the cation of MgATP. The self-consistency between some features of the homology model and the observations generated by PMK sequence alignment provides a rationale for conducting functional tests of the invariant basic (K17, R18, K19, K22) and acidic (D23) residues in this putative ATP binding loop region of the protein.

Biophysical Characterization of Human Phosphomevalonate Kinase Mutants. PMK mutants K17M, R18Q, K19M, K22M, and D23N have been expressed in soluble form at levels comparable to those of wild-type PMK and isolated in homogeneous forms (Figure 1). To test whether these mutants retained reasonable active site integrity (and, therefore, would be useful for more detailed characterization), the active site binding of a fluorescent ATP analogue, trinitrophenyl-ATP (TNP-ATP), was investigated. This fluorescent analogue is an alternate substrate for PMK. Enzyme turnover under comparable concentrations (200 μM) of TNP-ATP and ATP is reduced by 20-fold when the alternate substrate is used. The initial experiment with wild-type enzyme (Figure 5) indicated that the TNP-ATP probe binds efficiently to the protein, producing enhanced fluorescence and a spectral "blue" shift. Both wild-type (Figure 6) and mutant PMK proteins bind this substrate analogue (Table 3), although comparison between these proteins indicates modest differences ($\cong$3-fold; B_{max}) in fluorescence enhancement at saturating TNP-ATP, suggesting small variations in environment of the trinitrophenyl reporter group. Analysis of data from titration of these proteins with TNP-ATP suggests that there are not major differences in binding stoichiometries (0.8−1.4 per site) or in equilibrium binding constants (1.8−3.6 μM) between wild-type and mutant PMK proteins. On this basis, the ATP binding sites in the mutants seem to remain largely intact and exhibit no major perturbations that might complicate interpretation of kinetic characterization.

Kinetic Characterization of Human Phosphomevalonate Kinase Mutants. For the forward reaction (Table 1), mutagenic substitutions that eliminate charged side chains correlated with observation of only modest inflations in K_m values for ATP ($\leq$12-fold) and for mevalonate 5-phosphate ($\leq$7-fold). In the reverse reaction (Table 2), any observed

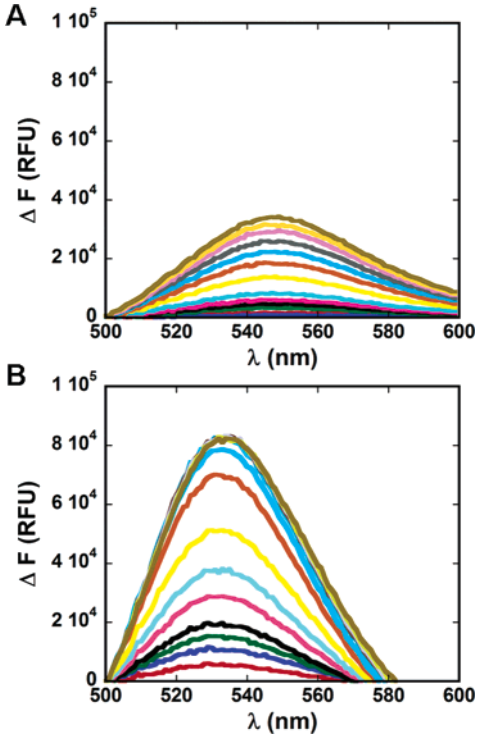

FIGURE 5: Fluorescence enhancement of TNP-ATP upon binding to PMK. Panel A displays the fluorescence ($\lambda_{max} \sim 545$ nm) obtained by titration of TNP-ATP (ranging from 0 to 10 μM) into buffer (100 mM MOPS, 100 mM KCl, 1 mM DTT, pH 7.0). Panel B displays the fluorescence ($\lambda_{max} \sim 535$ nm) obtained by titration of TNP-ATP into buffer containing 4.2 μM wild-type PMK. The excitation wavelength used in these experiments is 409 nm.

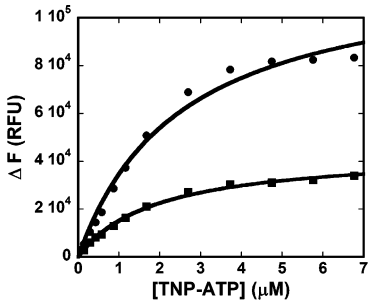

FIGURE 6: Titration of PMK with the fluorescent ATP analogue TNP-ATP. Fluorescence enhancement is displayed as a function of [TNP-ATP] for wild-type (●) and K22M (■) PMK. Data were fit by nonlinear regression analysis using the equation $y = [B_{max}(X)]/[K_d + (X)]$.

inflation in K_m values for either ADP or mevalonate 5-diphosphate was also modest (≤6-fold). Estimates of K_m parameters for the K22M mutant PMK were precluded by the diminished activity of this mutant. Use of a more sensitive spectrofluorometric method for the coupled assay allowed estimate for a specific activity for K22M in forward and reverse reactions but not measurements at subsaturating substrate concentrations. A major diminution in specific activity of $>10^4$-fold is observed in both forward (7.8×10^4-fold) and reverse (3.4×10^4-fold) reactions. Since binding affinity, as reflected by K_d for TNP-ATP, is not substantially influenced by the K22M mutation, the diminished catalytic activity suggests an active site assignment and a key role in phosphoryl transfer by PMK for the side chain of K22. For K19M and D23N, diminished V_{max} is most apparent for the reverse reaction. Additionally, the R18Q mutation primarily influences catalysis; decreases for V_{max} of 88-fold and 273-fold are observed for forward and reverse reactions, respectively. Of the multiple charged residues in PMK's highly conserved basic N-terminal sequence, these kinetic data most directly implicate R18 and K22 as functionally important residues.

Table 3: Comparison of Apparent Binding Constants for Wild-Type and Mutant PMK Enzymes to the Substrate Analogue TNP-ATP[a]

enzyme	n[b]	K_d (μM)[c]	B_{max} (RFU)
WT	0.90 ± 0.06	2.52 ± 0.35	122040 ± 7297
K17M	1.40 ± 0.02	3.02 ± 0.11	38772 ± 582
R18Q	1.40 ± 0.03	3.55 ± 0.15	53633 ± 1016
K19M	0.90 ± 0.02	3.00 ± 0.18	57729 ± 1365
K22M	1.00 ± 0.02	1.84 ± 0.11	43149 ± 837
D23N	0.80 ± 0.13	2.13 ± 0.60	121530 ± 20145

[a] Titrations of TNP-ATP to a fixed concentration of enzyme were done in 100 mM MOPS, 100 mM KCl, and 1 mM DTT (pH 7.0). [b] The n value (binding stoichiometry) was estimated by dividing the extrapolated B_{max} by the product of the enzyme concentration and the fluorescent enhancement corresponding to 1 μM bound probe. [c] K_d values were estimated by fitting the titration data to the equation $y = [B_{max}(X)]/[K_d + (X)]$.

DISCUSSION

The recombinant human phosphomevalonate kinase characterized in these studies represents an attractive protein model that can be useful for experiments aimed at generating functional correlations that cannot be inferred from observations derived using the divergent PMK proteins from plants, fungi, or bacteria. Results of amino acid sequence homology searches of protein databases indicate extended sequence alignments of human phosphomevalonate kinase with few proteins other than animal or invertebrate PMK proteins. This suggests that full-length homology of human PMK with other phosphotransferase proteins is not high. For this reason, the relationship between PMK and the nucleoside monophosphate kinases (specifically, phage deoxynucleotide kinase) that has been suggested by the homology model of the human PMK structure represents a potentially valuable observation. The model seems to be important to consider if its validity is supported by other experimental observations. The substantial amino acid sequence differences between PMK and other proteins in the nucleoside monophosphate kinase family are not unreasonable in the context of these enzymes' different phosphoryl acceptors (e.g., nucleotides versus nonnucleotide metabolites), different specific protein subunit contacts (for oligomeric proteins in this family), and potential binding sites for allosteric effectors. Despite the modest overall sequence identity between PMK and bacteriophage T4 deoxynucleotide kinase (≈24% for comparison of full-length protein chains), on the basis of a more extensive protein sequence profiling analysis, Leipe et al. (*11*) have argued that the sequence similarity is highly significant and that these enzymes have a common origin. Thus, the homology model for PMK structure may be useful in guiding future functional experiments or for corroborating results of empirical structural work. Some aspects of secondary structure (aside from the region proximal to the β sheet core) may not be well-defined in the model. For example, the nucleoside monophosphate kinase family of proteins typically exhibit LID regions (e.g., following β strand 4) that contain helical segments that harbor conserved basic residues

```
                                  10         20         30         40
                          ....|....| ....|....| ....|....| ....|....|
H. sapiens PMK            -----MAPLG GAPRLVLLFS GKRKSGKDFV TEALQSRLG-
Phage KVP40 dNMP kinase   ---------- ----MIIGIN GQKRSGKDTV AQAIQDIHS-
Phage phiC31 DNK          ---------- MAYYKSIGLI GRAQSGKDSV GARLRQRYG-
Phage T4 DNK              ---------- ---MKLIFLS GVKRSGKDTT ADFIMSNYS-
H. sapiens AK1            ------MEEK LKKTKIIFVV GGPGSGKGTQ CEKIVQKYG-
A. thaliana UMP/CMP kinase MGSVDAANGS GKKPTVIFVL GGPGSGKGTQ CAYIVEHYG-
S. cerevisiae GMP kinase  ---------- --MSRPIVIS GPSGTGKSTL LKKLFAEYPD
```

FIGURE 7: Sequence alignment of the N-terminal region of various nucleoside monophosphate kinase family members. The lysine observed in the N-terminal region of several nucleoside monophosphate kinases is boldfaced. All sequences were obtained from public databases. Alignment was generated using the BioEdit program (*37*). Sequences corresponding to the following organisms and accession numbers are included: *H. sapiens* (human) phosphomevalonate kinase, Q15126; bacteriophage KV40 deoxynucleoside monophosphate kinase, AAQ64394; bacteriophage phiC31 deoxynucleotide kinase, CAA07122; bacteriophage T4 deoxynucleotide kinase, P04531; *H. sapiens* (human) adenylate kinase 1, CAI12608; *A. thaliana* (thale cress) uridylate kinase/cytidylate kinase, AAB71135; *S. cerevisiae* (baker's yeast) guanylate kinase, P16454.

involved in substrate binding. The homology model for PMK is unstructured in this area, but it may be useful in drawing attention to several conserved residues in this region that could function in substrate binding as well-precedented LID movement brings them into proximity with the β sheet core of the protein.

If the protein fold predicted by the homology model of PMK is correct, some similarity should be expected in the ATP binding elements that are positioned adjacent to the parallel β strand core that is typical of this family of proteins. The mutagenesis results reported for human PMK as well as sequence alignments focused on the basic residue rich region are in accord with the predicted protein fold, which should contain an ATP site motif after an N-terminal β strand. The alignment (Figure 7) of the N-terminal region of PMK and several other members of the nucleoside monophosphate kinase family illustrates overall similarity that conforms to a consensus ATP binding loop [GxxxxGK-(S/T/D)] but also some interesting contrasts. Perhaps the most striking similarity with PMK is apparent upon comparison of PMK with bacteriophage T4 deoxynucleotide kinase; the structure of this enzyme is the template used for generating a homology model for PMK structure. Deoxynucleotide kinase (DNK) contains residues (K14, D15) homologous to PMK's K22 and D23 as well as two additional (K10, R11) basic residues, while PMK has three additional basic residues (K17, R18, K19) in this N-terminal region. While other phosphotransferases [such as adenylate kinase, uridylate/cytidylate (UMP/CMP) kinase, guanylate kinase] in the sequence alignment contain a lysine comparable to PMK K22, they contain no other basic or acidic residues. Protein modification experiments with bacteriophage T4 deoxynucleotide kinase (*25*) have implicated an active site lysine. Edman sequence analysis data were interpreted to suggest that the target of pyridoxal phosphate modification in that enzyme was a residue (K10) earlier in the sequence than the lysine (K14) that corresponds to PMK K22. Direct functional tests of the modification site in that protein by a mutagenesis approach have not been reported. In this context the results of PMK mutagenesis are useful in distinguishing between the contributions of the different lysine residues and argue for the dominant influence of K22 in comparison with K17 or K19.

The overall structure of deoxynucleotide kinase (DNK) proves to be useful in generating the homology model of PMK structure, but some details of DNK's active site view (*24*) are limited. For example, little electron density corresponding to cation or β- and γ-phosphoryls of MgATP substrate bound to this protein was observed, so modeling was used in interpreting and predicting active site interactions. On this basis, the lysine corresponding to PMK K22 is predicted to support ATP binding. Moreover, the deoxynucleotide kinase aspartate corresponding to PMK D23 is predicted to ligate the cation of MgATP in an atypical rigid bidentate mode and stimulate cleavage of ATP's γ-phosphoryl to an extent that was proposed to be detrimental to *cellular* phosphotransferases (*24*). Such a hypothesis needs to be reevaluated in view of the subsequent observation of a corresponding aspartate (D23) in PMK proteins. These new PMK sequence data indicate that such an acidic residue is not unique to *extracellular* (e.g., viral) phosphotransferases. Moreover, on the basis of mutagenesis results for human PMK, it is unclear that such an aspartate is critical to reactivity of ATP. Perhaps solvent water molecules mediate any postulated interaction of the carboxyl group of this conserved aspartate with the substrate, as observed for adenylate kinase (*26*, *27*), UMP kinase (*28*), and UMP/CMP kinase (*29*), all of which are also members of the nucleoside monophosphate kinase family.

Several nucleoside monophosphate kinase family proteins contain lysine residues that correspond to PMK's K22, but the influence of these lysines on catalytic function varies. A homologous lysine is present in plant UMP/CMP kinases (*30*). Substitution to eliminate the basic side chain correlates with a diminution in catalytic rate of only $\approx$5-fold (*31*). In contrast, mutagenesis of a comparable lysine in adenylate kinase [which uses a nucleotide phosphoryl acceptor (*32*, *33*)] reduces activity by $>10^4$-fold or in shikimate kinase [which uses a nonnucleotide phosphoryl acceptor (*34*)] reduces activity to nondetectable levels. The large effects reported for the latter two enzymes agree with the $>10^4$-fold effect measured for PMK K22M. For those enzymes in the nucleoside monophosphate kinase family that contain a Walker A motif lysine that is crucial to catalysis, it has been suggested (*35*, *36*) that this lysine stabilizes the transition state and provides a template that guides the γ-phosphoryl of ATP during an associative transfer to the acceptor substrate. Such a role would seem to be appropriate for K22 of human phosphomevalonate kinase.

ACKNOWLEDGMENT

We sincerely thank Dr. K. M. Gibson (Oregon Health Science University, Portland, OR) for providing human phosphomevalonate kinase cDNA.

REFERENCES

1. Hellig, H., and Popjak, G. (1961) Studies on the biosynthesis of cholesterol: XIII. phosphomevalonic kinase from liver, *J. Lipid Res. 2*, 235−243.
2. Lee, C. S., and O'Sullivan, W. J. (1985) Improved procedures for the synthesis of phosphomevalonate and for the assay and purification of pig liver phosphomevalonate kinase, *Biochim. Biophys. Acta 839*, 83−89.
3. Bazaes, S., Beytia, E., Jabalquinto, A. M., Solis de Ovando, F., Gomez, I., and Eyzaguirre, J. (1980) Pig liver phosphomevalone kinase. 1. Purification and properties, *Biochemistry 19*, 2300−2304.
4. Ku, E. C. (1996) Regulation of fatty acid biosynthesis by intermediates of the cholesterol biosynthetic pathway, *Biochem. Biophys. Res. Commun. 225*, 173−179.
5. Chambliss, K. L., Slaughter, C. A., Schreiner, R., Hoffmann, G. F., and Gibson, K. M. (1996) Molecular cloning of human phosphomevalonate kinase and identification of a consensus peroxisomal targeting sequence, *J. Biol. Chem. 271*, 17330−17334.
6. Hinson, D. D., Chambliss, K. L., Toth, M. J., Tanaka, R. D., and Gibson, K. M. (1997) Post-translational regulation of mevalonate kinase by intermediates of the cholesterol and nonsterol isoprene biosynthetic pathways, *J. Lipid Res. 38*, 2216−2223.
7. Smit, A., and Mushegian, A. (2000) Biosynthesis of isoprenoids via mevalonate in Archaea: the lost pathway, *Genome Res. 10*, 1468−1484.
8. Wilding, E. I., Brown, J. R., Bryant, A. P., Chalker, A. F., Holmes, D. J., Ingraham, K. A., Iordanescu, S., So, C. Y., Rosenberg, M., and Gwynn, M. N. (2000) Identification, evolution, and essentiality of the mevalonate pathway for isopentenyl diphosphate biosynthesis in gram-positive cocci, *J. Bacteriol. 182*, 4319−4327.
9. Romanowski, M. J., Bonanno, J. B., and Burley, S. K. (2002) Crystal structure of the *Streptococcus pneumoniae* phosphomevalonate kinase, a member of the GHMP kinase superfamily, *Proteins 47*, 568−571.
10. Pilloff, D., Dabovic, K., Romanowski, M. J., Bonanno, J. B., Doherty, M., Burley, S. K., and Leyh, T. S. (2003) The kinetic mechanism of phosphomevalonate kinase, *J. Biol. Chem. 278*, 4510−4515.
11. Leipe, D. D., Koonin, E. V., and Aravind, L. (2003) Evolution and classification of P-loop kinases and related proteins, *J. Mol. Biol. 333*, 781−815.
12. Wang, C. Z., and Miziorko, H. M. (2003) Methodology for synthesis and isolation of 5-phosphomevalonic acid, *Anal. Biochem 321*, 272−275.
13. Reardon, J. E., and Abeles, R. H. (1987) Inhibition of cholesterol biosynthesis by fluorinated mevalonate analogues, *Biochemistry 26*, 4717−4722.
14. Laemmli, U. K. (1970) Cleavage of structural proteins during the assembly of the head of bacteriophage T4, *Nature 227*, 680−685.
15. Liu, F., Dong, Q., Myers, A. M., and Fromm, H. J. (1991) Expression of human brain hexokinase in *Escherichia coli*: purification and characterization of the expressed enzyme, *Biochem. Biophys. Res. Commun. 177*, 305−311.
16. Tchen, T. T. (1962) Enzymes in sterol biogenesis, *Methods Enzymol. 5*, 489−499.
17. Hiratsuka, T., and Uchida, K. (1973) Preparation and properties of 2′(or 3′)-O-(2,4,6-trinitrophenyl) adenosine 5′-triphosphate, an analog of adenosine triphosphate, *Biochim. Biophys. Acta 320*, 635−647.
18. Kelley, L. A., MacCallum, R. M., and Sternberg, M. J. E. (2000) Enhanced genome annotation using structural profiles in the program 3D-PSSM, *J. Mol. Biol. 299*, 499−520.
19. Laskowski, R. A., MacArthur, M. W., Moss, D. S., and Thornton, J. M. (1993) PROCHECK: a program to check the stereochemical quality of protein structures, *J. Appl. Crystallogr. 26*, 283−291.
20. Eyzaguirre, J., and Bazaes, S. (1985) Phosphomevalonate kinase from pig liver, *Methods Enzymol. 110*, 78−85.
21. Lee, C. S., and O'Sullivan, W. J. (1985) The interaction of phosphorothioate analogues of ATP with phosphomevalonate kinase. Kinetic and ^{31}P NMR studies, *J. Biol. Chem. 260*, 13909−13915.
22. Bloch, K., Chaykin, S., Phillips, A. H., and De Waard, A. (1959) Mevalonic acid pyrophosphate and isopentenylpyrophosphate, *J. Biol. Chem. 234*, 2595−2604.
23. Henning, U., Moslein, E. M., and Lynen, F. (1959) Biosynthesis of terpenes. V. Formation of 5-pyrophosphomevalonic acid by phosphomevalonic kinase, *Arch. Biochem. Biophys. 83*, 259−267.
24. Teplyakov, A., Sebastiao, P., Obmolova, G., Perrakis, A., Brush, G. S., Bessman, M. J., and Wilson, K. S. (1996) Crystal structure of bacteriophage T4 deoxynucleotide kinase with its substrates dGMP and ATP, *EMBO J. 15*, 3487−3497.
25. Brush, G. S., and Bessman, M. J. (1993) Chemical modification of bacteriophage T4 deoxynucleotide kinase. Evidence of a single catalytic region, *J. Biol. Chem. 268*, 1603−1609.
26. Krishnamurthy, H., Lou, H., Kimple, A., Vieille, C., and Cukier, R. I. (2005) Associative mechanism for phosphoryl transfer: a molecular dynamics simulation of *Escherichia coli* adenylate kinase complexed with its substrates, *Proteins 58*, 88−100.
27. Abele, U., and Schulz, G. E. (1995) High-resolution structures of adenylate kinase from yeast ligated with inhibitor Ap(5)A, showing the pathway of phosphoryl transfer, *Protein Sci. 4*, 1262−1271.
28. Muller-Dieckmann, H. J., and Schulz, G. E. (1994) The structure of uridylate kinase with its substrates, showing the transition state geometry, *J. Mol. Biol. 236*, 361−367.
29. Scheffzek, K., Kliche, W., Wiesmuller, L., and Reinstein, J. (1996) Crystal structure of the complex of UMP/CMP kinase from *Dictyostelium discoideum* and the bisubstrate inhibitor P1-(5′-adenosyl) P5-(5′-uridyl) pentaphosphate (UP5A) and Mg^{2+} at 2.2 Å: Implications for water-mediated specificity, *Biochemistry 35*, 9716−9727.
30. Zhou, L., Lacroute, F., and Thornburg, R. (1998) Cloning, expression in *Escherichia coli*, and characterization of *Arabidopsis thaliana* UMP/CMP kinase, *Plant Physiol. 117*, 245−254.
31. Zhou, L., and Thornburg, R. (1998) Site-specific mutations of conserved residues in the phosphate-binding loop of the Arabidopsis UMP/CMP kinase alter ATP and UMP binding, *Arch. Biochem. Biophys. 358*, 297−302.
32. Tian, G. C., Yan, H. G., Jiang, R. T., Kishi, F., Nakazawa, A., and Tsai, M. D. (1990) Mechanism of adenylate kinase. Are the essential lysines essential?, *Biochemistry 29*, 4296−4304.
33. Reinstein, J., Schlichting, I., and Wittinghofer, A. (1990) Structurally and catalytically important residues in the phosphate binding loop of adenylate kinase of *Escherichia coli*, *Biochemistry 29*, 7451−7459.
34. Krell, T., Maclean, J., Boam, D. J., Cooper, A., Resmini, M., Brocklehurst, K., Kelly, S. M., Price, N. C., Lapthorn, A. J., and Coggins, J. R. (2001) Biochemical and X-ray crystallographic studies on shikimate kinase: The important structural role of the P-loop lysine, *Protein Sci. 10*, 1137−1149.
35. Schlichting, I., and Reinstein, J. (1997) Structures of active conformations of UMP kinase from *Dictyostelium discoideum* suggest phosphoryl transfer is associative, *Biochemistry 36*, 9290−9296.
36. Shulz, G. E. (1992) Binding of nucleotides by proteins, *Curr. Opin. Struct. Biol. 2*, 61−67.
37. Hall, T. A. (1999) BioEdit: A user-friendly bilogical sequence alignment editor and analysis program for Windows 95/98/NT, *Nucleic Acids Symp. Ser. 41*, 95−98.

BI052231U